Materials Today Communications 26 (2021) 101716

Contents lists available at ScienceDirect

Materials Today Communications

journal homepage: www.elsevier.com/locate/mtcomm

High electrochemical detection of dopamine based on Cu doped single phase hexagonally ZnO plates

Azam Anaraki Firooz [a,b,*], Masoumeh Ghalkhani [a,*], Jimmy A. Faria Albanese [b], Maryam Ghanbari [a]

[a] Department of Chemistry, Faculty of science, Shahid Rajaee Teacher Training University, Tehran, Iran
[b] Catalytic Processes and Materials Group, Faculty of Science and Technology, MESA+ Institute for Nanotechnology, University of Twente, PO Box 217, 7500 AE, Enschede, the Netherlands

ARTICLE INFO

Keywords:
Cu doping
ZnO
Dopamine
Hydrothermal
Voltammetric, Electrode

ABSTRACT

Dopamine is a chemical that plays a key role in various neurological diseases such as Parkinson's, depression, and some types of cancer. Hence, sensitive detection methods of dopamine are necessary for early discernment of diseases related to abnormal levels. In this study, Cu doped ZnO (Cu/ZnO) nanostructures, immobilized onto the surface of glassy carbon electrode (GCE), have been investigated as a highly efficient electrode material for the electrochemical detection of dopamine (DA). A simple hydrothermal process was used for the synthesis of the ZnO and Cu/ZnO nanostructures. Detailed characterization revealed that addition of Cu on the ZnO changed the morphology of ZnO creating a highly microporous nanostructure. The electrochemical response of DA on the Cu/ZnO/GC electrodes, determined using cyclic voltammetry (CV) and differential pulsed voltammetry (DPV), indicated that on these materials it is possible to achieve lower over-potentials for the DA oxidation and higher catalytic activity. Furthermore, the GCE modified with 50 % Cu doped ZnO showed the most promising performance with high stability in wide range of pH values (2–8 pH), and linear response for DA from 0.1–20 μM with high sensitivity of 2630 nA/μM and detection limit as low as 55 nM. The analytical performance of the developed sensor showed its potential capability for the DA quantification in complex biological systems.

1. Introduction

Dopamine (DA) is one of the brain's neurotransmitters that ferries information between neurons [1–3]. Consequently, abnormal DA levels result in some neurological disorders such as schizophrenia and Parkinson's disease [4,5]. Therefore, for the detection of DA, various techniques have been used such as photospectrometry, chromatography and mass spectrometry [6]. However, the electrochemical technique is preferred due to its easy and low cost utilization, high sensitivity, time effectiveness, and low detection limit [7,8].

One of the challenges in detecting DA by electrochemical method is the proximity of its oxidation potential to some other biological compounds, such as ascorbic acid (AA) and uric acid (UA), and another one is contamination of the electrode surface due to the adsorption of oxidation products. As a result, the electrode's efficiency is reduced in detection [9,10]. Therefore, in order to overcome this problem, it is better to use the modified electrodes. The advantages of modified electrode surfaces can be noted: transfer of the improving physical and chemical properties of the modifier to the electrode, more electrical activity due to the use of materials with a large surface area and proving higher selectivity in detection. Thus, greater sensitivity and selectivity can be achieved by the use of modified electrodes [11,12].

The factors influencing the modified electrode response can include the nature of the modifier material, the method of modifier synthesis, the electrode coating mechanism and the use of intermediates, and the nature of the sample matrix. Glassy carbon electrode (GCE) is one of the most commonly used electrodes to modify because it provides a wide potential window and is chemically stable. GCE was mostly used as modified electrode substrate for biosensing of DA as compared to Pt, graphite and gold electrode [13–15].

Today, application of metal oxide nanoparticles as the electrode modifier instead of their bulk materials are particularly noteworthy due to the major advantages, including cost effective, enhanced electron transfer kinetics, higher specific surface area, and higher electrocatalytic activity, and selectivity [15].

Among these metal oxides, nanostructured ZnO has been extensively

* Corresponding authors at: Department of Chemistry, Faculty of science, Shahid Rajaee Teacher Training University, Tehran, Iran.
E-mail addresses: azam_a_f@yahoo.com (A. Anaraki Firooz), ghalkhani@sru.ac.ir (M. Ghalkhani).

https://doi.org/10.1016/j.mtcomm.2020.101716
Received 29 June 2020; Received in revised form 6 September 2020; Accepted 18 September 2020
Available online 1 October 2020

used as the electrode modifier due to specific properties including high surface area, thermal stability, the biocompatible nature, wide band gap, and fast electron transfer kinetics. Moreover, higher surface area of this material makes it very effective for the adsorption of analytes like DA [16–19].

Notably, there are some studies on hybrid nanostructures of ZnO that showed higher catalytic activity and fast electron transfer ability to the supporting electrodes [20–22], properties that are essential for high sensitivity and accuracy of the sensor. Besides ZnO, copper have been well-studied as an efficient catalytic material in applications as diverse as selective oxidation of hydrocarbons [23,24], methanol synthesis [25, 26], electrochemical sensing [27–29], photocatalysis [30]. These base metal oxides are inexpensive and their synthesize protocols involve mild reaction conditions that facilitate scaling-up the fabrication, while preserving the high tunability of their electrochemical and catalytic activity, selectivity and stability [31,32]. While the work conducted on ZnO-based electrodes for dopamine detection (DA) has led to significant advancements, these materials have shown low sensitivity (see Table 1) 0.09–317.8 nA/μM. This is a relevant issue as the normal extracellular concentration of DA ranges from 10^{-5} to 10^{-3} mM in healthy individuals [16,18,33–35]. Thus, new synthesis strategies and hybrid material compositions are needed to enable practical implementation of these electrodes in DA electrochemical sensing.

To tackle this challenge, we have synthesized ZnO and Cu doped ZnO nanostructures on Glassy Carbon Electrode (GCE) by a simple hydrothermal crystallization method at low temperature. Our results indicate that these nanostructures have extremely high sensitivity and stability with low detection limit towards DA. The sensor is fabricated easily, cost effective, and could be used for usual determining of DA in biological systems.

2. Experimental

2.1. Materials and reagents

All materials utilized in present work were of analytical reagent grade from Merck. A prepared stock solution of Britton–Robinson (BR) buffer comprising 0.04 M of glacial acetic acid, orthophosphoric acid and boric acid was employed as the supporting electrolyte in voltammetric experiments. 0.1 M NaOH solution was used for adjusting the pH of burred solutions.

2.2. Apparatus

Voltammetric tests were performed by a SAMA 500 electroanalyzer system, I. R. Iran. An electrochemical cell was used with a glassy carbon working electrode (d =2.0 mm, received from Azar Electrode Co., Urmia, I.R. Iran), saturated calomel reference electrode (SCE) and a Pt rod auxiliary electrode. Other employed instruments for pH measurement, modifier suspension preparation and characterization of the synthesized materials were as reported in our previous work [36].

2.3. Synthesis and characterization of nanomaterials

According to our previous research, ZnO and Cu doped ZnO structures were prepared by hydrothermal method and the concentration of Cu dopants was 15 % and 50 % of Zn (mole ratio of dopant to Zn is 15 and 50 %, respectively). 5 mmol $Zn(Ac)_2.2H_2O$ and 10 mmol ribose were dissolved in 50 ml distilled water, were mixed and the stirring was continued for 30 min at room temperature. After stirring, adequate mmol of cupric acetate added to solution and again stirred for 30 min. After that time, 10 mmol NaOH added to solution. The achieved solution was then transferred to Teflon lined autoclave, and sealed and heated up to 90 °C for 2 h. After completion of the reaction, the autoclave was allowed to cool at room temperature followed by washing with water serially and dried at room temperature. The samples before and after

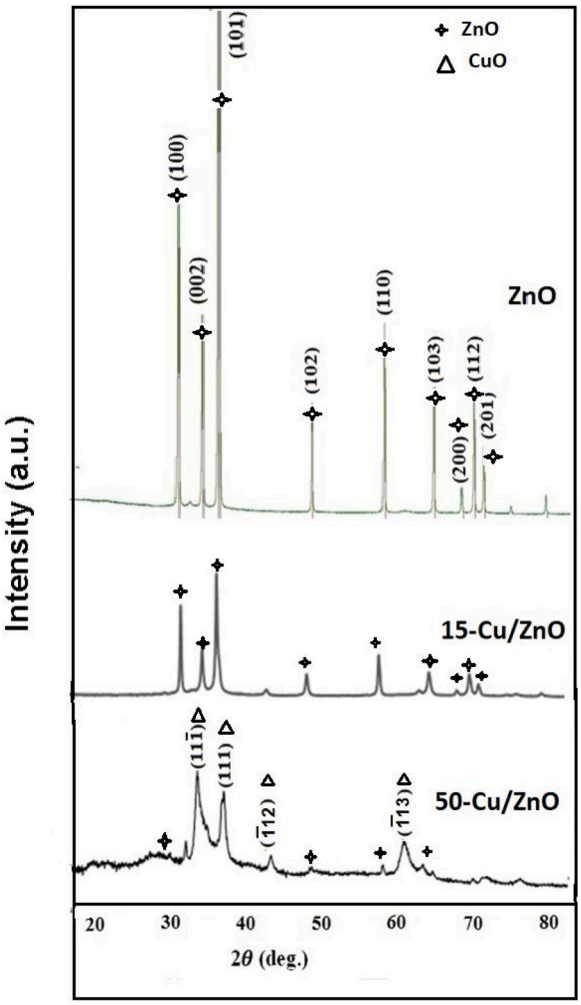

Fig. 1. XRD of the samples.

doping with mole ratio of dopant to Zn, 15 and 50 %, were donated as ZnO, 15-Cu/ZnO and 50-Cu/ZnO, respectively. The morphology and size of the products were characterized by scanning electron microscopy (SEM Holland Philips XL30). The crystalline phase was determined by powder X-ray diffraction (XRD using the Cu Kα wavelength of 1.5405A). The ultraviolet–visible (UV–vis) absorption spectra were measured on a spectrophotometer (Rayleig).

2.4. Preparation of modified electrode

Initially, the GCE electrode was sonicated for 8 min in distilled water and then polished with slurry of the 0.05 μm alumina powder to make the surface of the electrode completely polished and mirrored. To be ensured that the GCE surface is cleaned, it is consecutive cycled in the electrolyte solution until obtained low and stable background current. Suspension of each nanoparticle was prepared by dissolving 3 mg of the synthesized nanoparticles in mixture solution of 1 ml water and 2 ml DMF and stirred for 60 min. Then, required microliter of the prepared suspensions was drop casted onto the GCE surface and let dry in an oven at 65 °C for 10 min.

3. Result and discussion

3.1. Characterization of the synthesized nanostructures

In this study, we develop a simple and green route to synthesize the ZnO, 15-Cu/ZnO and 50-Cu/ZnO nanostructures via hydrothermal,

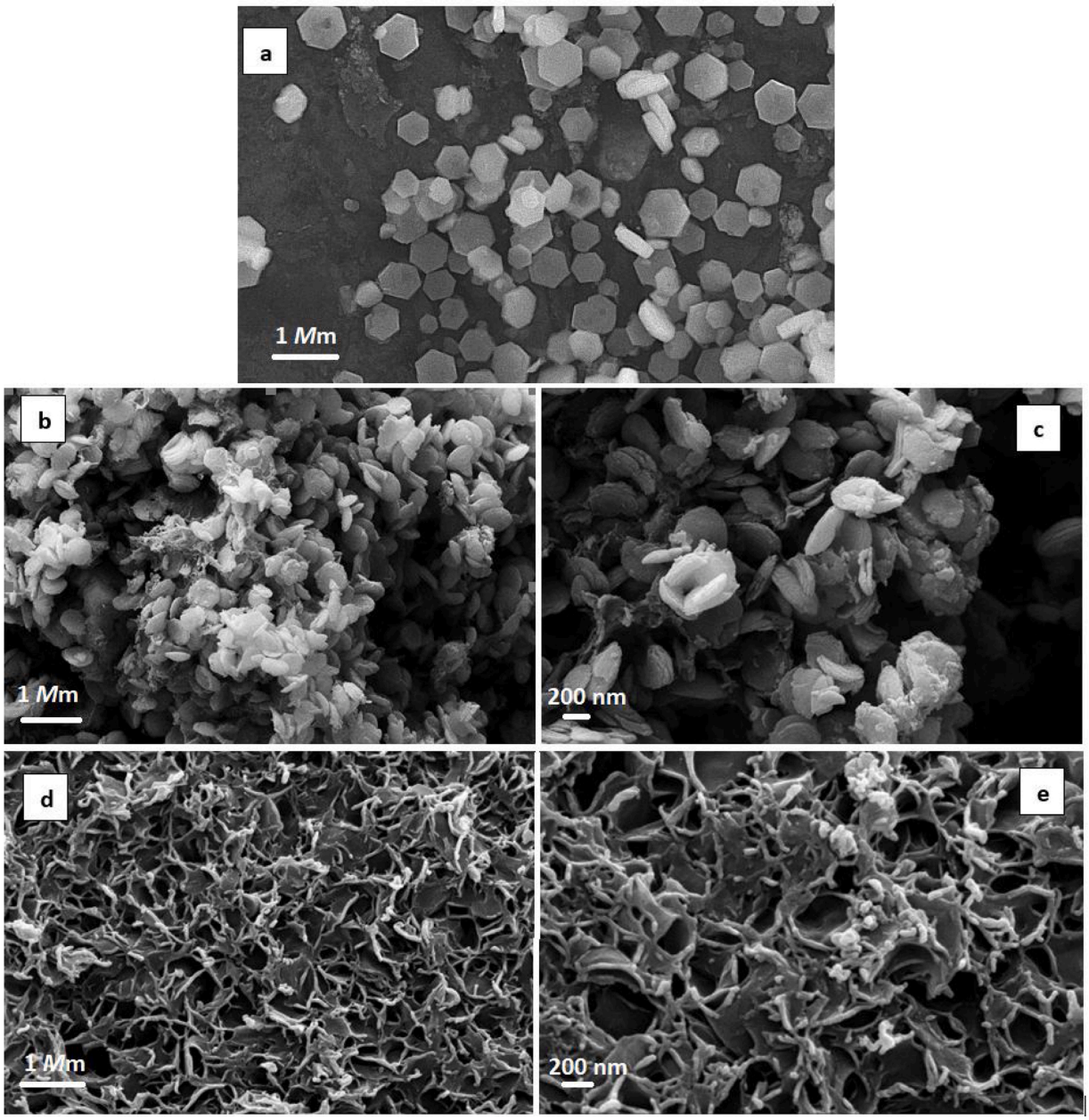

Fig. 2. SEM images of a) ZnO, b) 15- Cu/ZnO, c) 50- Cu/ZnO at low magnification, and d) 15- Cu/ZnO and e) 50- Cu/ZnO samples at higher magnification.

using zinc acetate, NaOH as precursors, cupper acetate as dopants, H_2O as solvent and ribose as template at low temperature. We employed an environmentally friendly synthesis technique.

In order to determine the crystalline structures of the nanostructures, X-ray diffraction (XRD) is performed. Fig. 1 shows the XRD patterns of the ZnO, 15-Cu/ZnO and 50-Cu/ZnO nanostructures. As shown in Fig. 1a, XRD patterns of the ZnO are correspond to wurtzite hexagonal phase of ZnO in accordance with the JCDPS card 36-1451. Fig. 1b shows XRD patterns of 15-Cu/ZnO sample. No reflections characteristic related to Cu and other impurities is observed in its patterns. It is may be due to replacement of Cu ions in the lattice of ZnO or formed Cu crystallites are too small to be detected via XRD [37]. Moreover, with addition of Cu, intensity of the diffraction peaks decreases, indicating formation of smaller crystallites size.

While, when the molar ratio of Cu/Zn is 50 % in the reaction system, the XRD patterns contain diffraction peaks from both wortzite ZnO and monoclinic CuO. As shown in Fig. 1c, planes at 2-thetha degree at 35.5° and 38.7° are belonged to (11ī) and (111), respectively. These peaks confirm that the 50-Cu/ZnO nanostructure contains CuO with monoclinic structure beside wortzite ZnO.

Fig. 2 shows the typical SEM images of the synthesized structures with using different ratio of Cu. As shown in this Fig. without using any dopands, ZnO structures with single phase hexagonally plate ZnO microstructure morphology obtained (Fig. 2a) [38]. Diameter and widths of these hexagonal plates are in range of 400−1200 nm and ~250 nm, respectively.

Incorporating copper acetate in a molar ratio of 15 % in the reaction system results in the products relatively uniform roundlet sheets (Fig. 2b), which comprise of numerous nanoparticles (Fig. 2c). The diameters and widths of these roundlet sheets are in range of 300−500 nm and ~30−50 nm, respectively. Notably, by increasing further the copper acetate in the reaction system to 50 %, highly porous nanostructures were obtained (Fig. 2d and 2f).

The characterization of the chemical composition of the different catalysts was studied by Energy Dispersive X-rays spectroscopy (EDX) (see Fig. 3). While this technique allows detailed characterization of

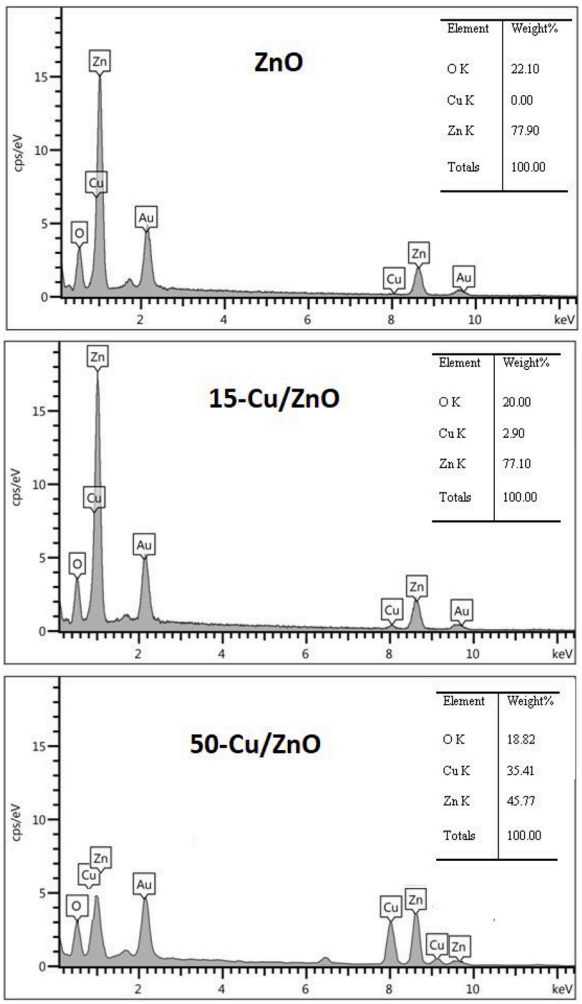

Fig. 3. EDX of the samples.

nanostructure materials when combined with Scanning Electron Microscopy (SEM), the atomic composition results obtained are strongly influenced by the penetration depth of the incoming X-rays in the inspected region of the sample [39]. Thus, this is often regarded as a semi-quantitative method for chemical composition analysis at nano-scales. As it can be noted in Fig. 3a, in the ZnO sample the peaks corresponding to the Zn and O K-electronic transition are observed together with the gold overcoating employed to increase the sample electrical conductivity and avoid surface charging. Upon addition of Cu in system, the K-transition of the Cu atoms are observed. The atomic composition analysis reveals an increase of the Cu content from 2.9 to 35 % for the 15-Cu/ZnO and 50-Cu/ZnO samples, respectively (Figs. 3b and 3c). The deviations in the Cu atomic content could be attributed to the heterogeneity of the samples, in which spatial overlap between CuO phases embedded on ZnO matrix result in large deviations from the real compositions.

Fig.4 shows the schematic diagram of the growth mechanism of our synthesized materials based on the SEM and XRD results. According to our previous research [36], when zinc acetate is mixed with NaOH, $Zn(OH)_2$ precipitates are formed. In higher concentration of NaOH, some of the insoluble $Zn(OH)_2$ will transform to soluble $[Zn(OH)_4]^{2-}$ ions. $Zn(OH)_2$ and $[Zn(OH)_4]^{2-}$ are responsible for the homogeneous nucleation and crystal growth of ZnO, respectively. Moreover, the presence of ribose as the template in the reaction system modifies the behavior of the −OH- by increasing the adsorption of these ions instead of the $[Zn(OH)_4]^{2-}$ ions. Since OH- ions prefer to adhere to the polar faces of the (001) crystal with respect to the nonpolar faces (100), shielding of the polar faces occurs [37,38]. As a result, preferential crystal growth in the [100] direction occurs leading to ZnO with hexagonally plate morphology.

Upon addition of copper acetate in reaction system, dissolved Cu^{+2} ions form intermediate $[Cu(OH)_2]$ aggregates. These aggregates change the availability of the hydroxyl groups on the surface of the growing ZnO core. In this case, the nucleation rate is fast, while the crystal growth rate is slow. So, particles with relatively small size are obtained. With increasing concentrations of copper acetate in reaction system (molar ratio of Cu/Zn is 50 %), the nucleation rate is faster and CuO nanostructures protruded on the ZnO nanostructures (Fig. 4).

3.2. Electrochemical characterization of prepared electrodes

At first, the effective surface area of the bare GCE and the GCE modified with ZnO, 15-Cu/ZnO and 50-Cu/ZnO nano-compounds was evaluated. The CV response of mentioned electrodes was compared in a 0.1 M KCl solution containing 1 mM $K_3Fe(CN)_6$. Obtained results showed that the effective surface area of the GCE was increased after covering its surface with synthesized ZnO nanostructures. Then, we evaluated the impedance changes of the bare electrode after

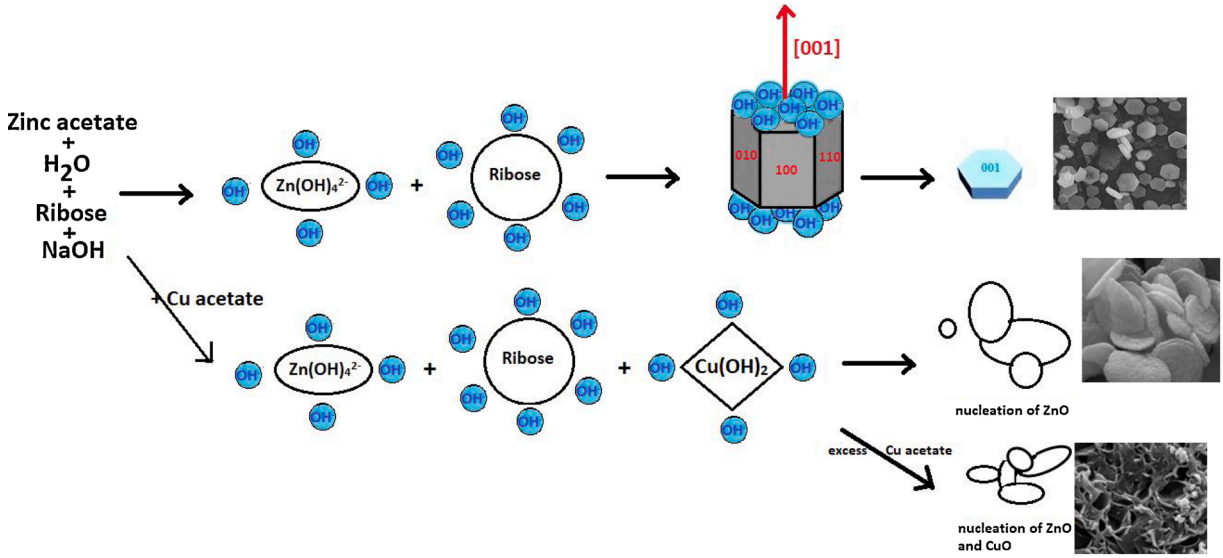

Fig. 4. Proposed mechanism for the formation of the nanostructures.

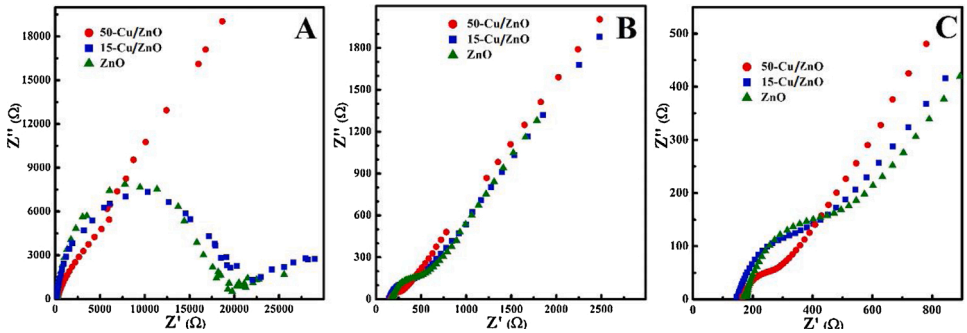

Fig. 5. Nyquist plots (Z″ *vs.* Z′) for the EIS measurements in 1.0 mM $K_3[Fe(CN)_6]$/ $K_4[Fe(CN)_6]$ for (A) as prepared and (B) activated ZnO/GCE (▲)15-Cu/ZnO/GCE (■) and 50-Cu/ZnO/GCE (●) in 0.1 M NaOH solution by 20 successive CV scan. (C) Magnification of the high frequency part of the impedance spectra in (B).

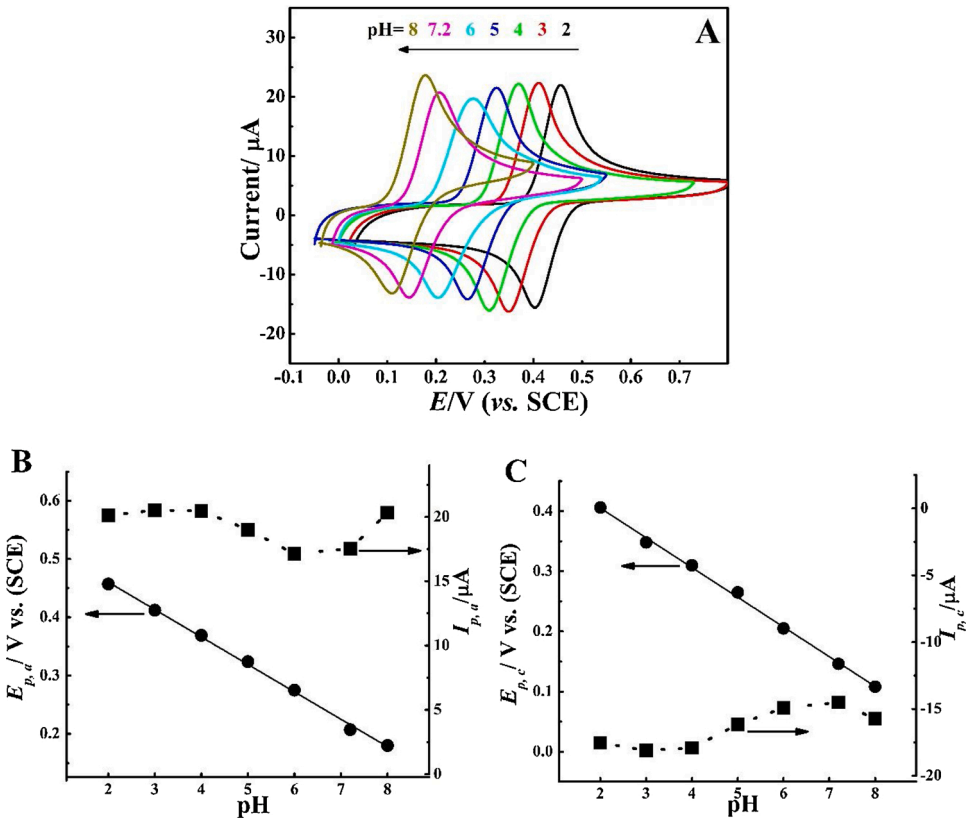

Fig. 6. (A) CVs of 100 μM DA on ZnO/GCE in solutions with different pHs (2–8). Plots of (B) $E_{p,a}$ and $I_{p,a}$ and (C) $E_{p,c}$ and $I_{p,c}$ *vs.* pH; scan rate was 100 mV/s.

modification with synthesized ZnO based nanostructures using electrochemical impedance spectroscopy (EIS). Fig. 5A shows the Nyquist plots of 1.0 mM $K_3[Fe(CN)_6]$/ $K_4[Fe(CN)_6]$ as redox probe at the as prepared GCE modified with nano ZnO, 15-Cu/ZnO and 50-Cu/ZnO. A very large semicircle with a diameter of about 20 KΩ was obtained at ZnO/GCE, 15-Cu/ZnO/GCE revealing high resistances of the semi conductive nano ZnO materials, which restrict the charge transfer process at the interface of electrode surface-solution. Meanwhile, after electrochemically activating the prepared modified electrodes by applying successive CVs in alkaline solution the semicircle vanishes significantly, Fig. 5B and C. This observation reveals the enhancement of electrical conductivity of the ZnO based modified GCEs, which are more suitable for electroanalytical purposes.

3.3. The influence of pH

The CV response of 100 μM DA buffered solutions with various pH in the range of 2–8 was recorded, Fig. 6A. As shown in Figs. 6B and 6C, by increasing the pH of buffer solution the oxidation and reduction peaks potential of DA were negatively shifted, revealing the involvement of proton ions in the redox reaction of DA at ZnO/GCE.

$$E_{p,a} = -0.047\,pH + 0.554 (R2 = 0.998,\ E_{p,a}: V) \quad (1)$$

$$E_{p,c} = -0.050\,pH + 0.504 (R2 = 0.998,\ Ep,c: V) \quad (2)$$

The $E_{p,a}$ and $E_{p,c}$ were displaced linearly according to the Eq. (1) and (2). The slopes of -0.047 and -0.050 V/pH demonstrate involvement of two-protons and two-electrons in redox reaction of DA at ZnO/GCE. Fig. 7, shows the graphical representation of the mechanism for electrochemical oxidation of DA at modified Cu/ZnO/GCE, which is consistent with previous literatures [40,41].

The redox peak currents of DA were varied in evaluated pH range with maximum values obtained at pH 3. It is worthy to mention that DA undergoes self-polymerization in alkaline environment in the presence

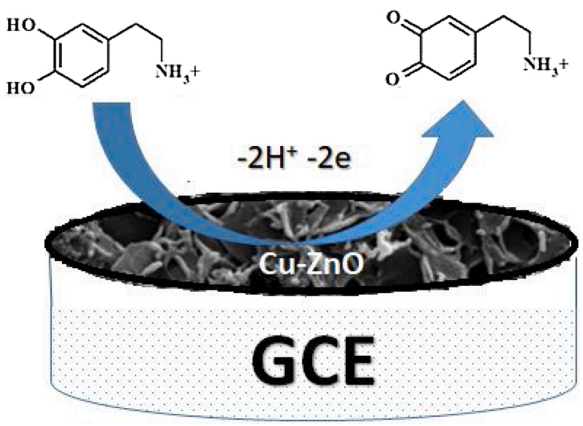

Fig. 7. Proposed mechanism for DA electro-oxidation at 50-Cu/ZnO/GCE in pH 2.0.

of oxygen, so the neutral and acidic solution of DA are more stable. In addition, in case of DA oxidation, the Michael addition process is taking place at DA solution with pH value higher than its pK_a and the mechanism of the redox reaction changes from simple electrochemical reversible process to the Electrochemical-Chemical-Electrochemical (ECE) mechanism.

3.4. Study of the electrochemical behavior of DA

The CV and DPV responses of prepared electrodes, after activation in alkaline solution, towards 100 μM DA in BR buffered solution of pH 7 were shown in Fig. 8A and C. A broad difference was observed for the anodic and cathodic peaks potential of DA with small peak currents at GCE. Meanwhile, a substantial negative and positive shift was observed for the oxidation and reduction peaks of DA, respectively, at the modified electrodes confirming the reduction of over-potential of redox reaction of DA due to electrocatalytic effect of the synthesized ZnO based

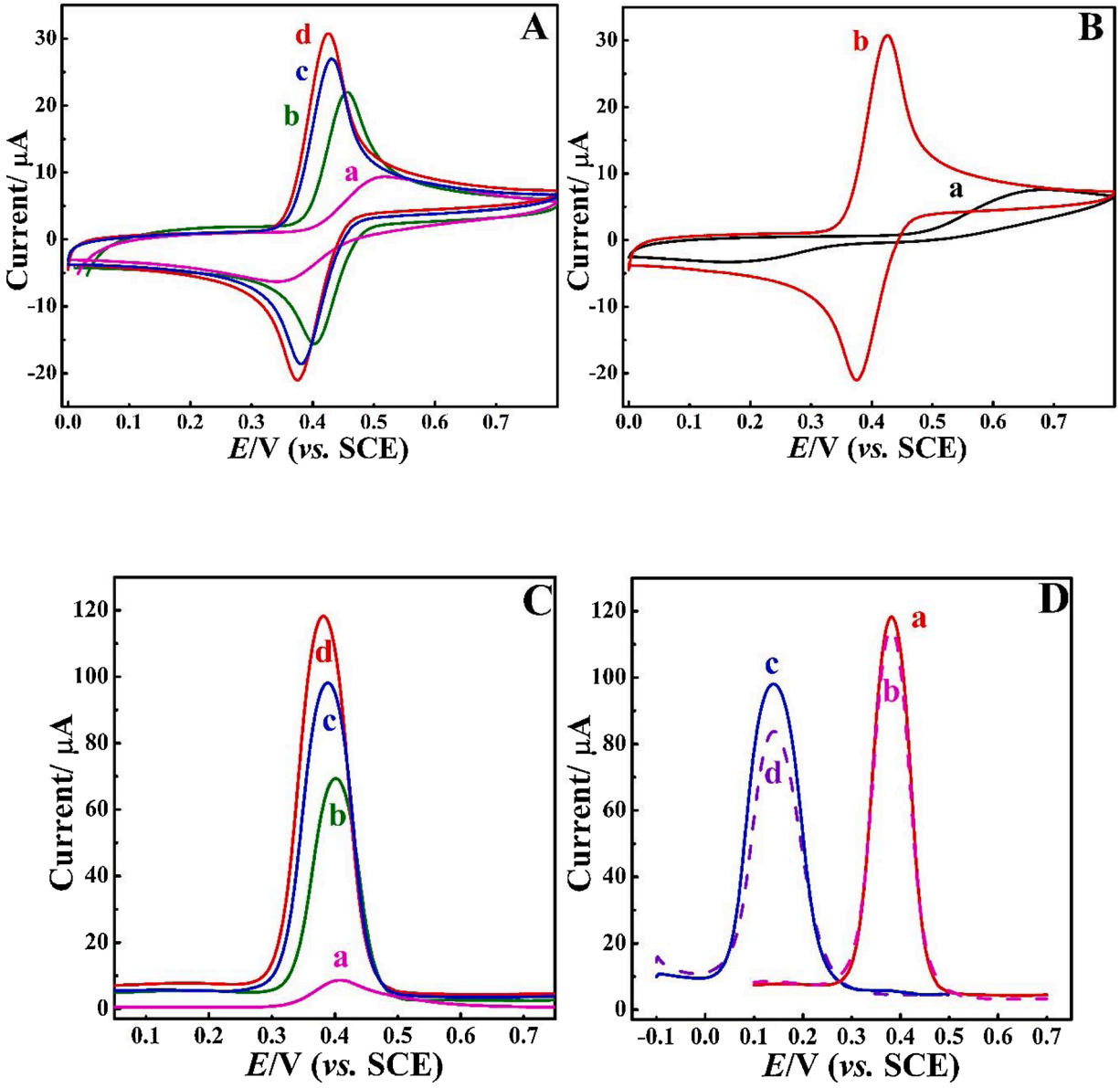

Fig. 8. CVs (A) and DPVs (C) of 100 μM DA at (a) bare GCE, (b) ZnO/GCE, (c) 15-Cu/ZnO/GCE and (d) 50-Cu/ZnO/GCE; all electrodes were electro-activated in alkaline solution before testing in DA solution. (B) CVs of 100 μM DA at 50-Cu/ZnO/GCE before (a) and after electro-activation (b); in 0.04 M BR buffer solution (pH 2.0) scan rate 100 mV s^{-1}. (D) Two successive DPVs for 50-Cu/ZnO/GCE after electro-activation in 100 μM DA in 0.04 M BR buffer solution of (a and b) pH 2.0 and (c, d) pH 7.0.

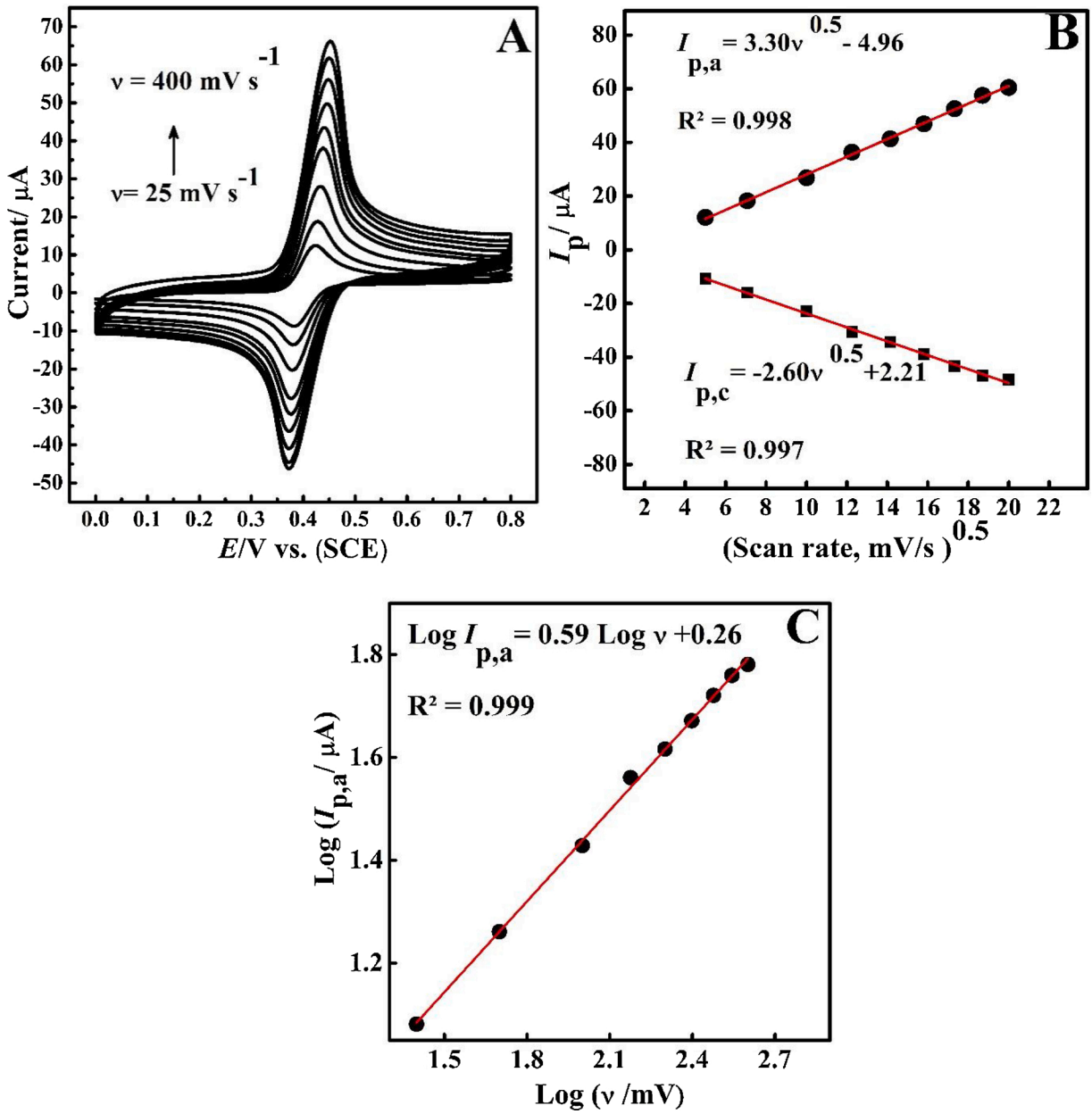

Fig. 9. (A) CVs of 100 μM DA at 50-Cu/ZnO/GCE at different scan rates in 0.04 M BR solution (pH 2.0). The plot of (B) $I_{p,a}$ (•) and $I_{p,c}$ (■) versus $\upsilon^{0.5}$ and (C) Log $I_{p,a}$ versus Log (υ).

nano-materials [42]. The increment observation of the redox peaks current of DA at ZnO/GCE, 15-Cu/ZnO/GCE and 50-Cu/ZnO/GCE compared to the bare GCE, reveals the enhancement of the effective surface area.

The obtained results demonstrate that by doping the Cu in the structure of the nano-ZnO, the over-potentials of the DA oxidation decreased confirming the effective electro-catalytic effect of Cu dopant. In comparison to ZnO/GCE, the Cu doped ZnO modified GCEs showed higher peak currents. The increasing the Cu doping percentage from 15 to 50 % led to enhancement of DA oxidation peak current from 25.42 to 29.55 μA in CV test and 93.84–1123.3 in DPV test. Therefore, it can be concluded that doping of Cu in ZnO nano-structure enhances its electro-catalytic role. Notably, the SEM images of the synthesized nano-structures showed a porous morphology for 50-Cu/ZnO that reveals its high effective surface area. Therefore, the 50-Cu/ZnO/GCE was chosen for further investigations.

Fig. 8B shows the recorded CVs of as prepared 50-Cu/ZnO/GCE and after its activation in alkaline solution in 100 μM DA solution of pH 2. An irreversible redox peaks were observed for DA electrochemical oxidation at inactivated 50-Cu/ZnO/GCE for which ΔE_p of 520 mV and $I_{p,c}/I_{p,a}$ of 0.3 were obtained, which are lower than those observed in case of bare GCE. However, the cycling the as prepared 50-Cu/ZnO/GCE in 0.1 M alkaline solution effectively activated the electrode surface after which the ΔE_p of DA redox peaks was significantly reduced to 50 mV and Ip,c/Ip,a increased to 0.83. These observations revealed that we must activate the GCE modified with ZnO based nanostructures in alkaline solution before performing main voltammetric experiments to enhance its electrocalytic activity.

Fig. 8D shows the two successive DPVs recorded in 100 μM DA solution of pH 2 and 7 using 50-Cu/ZnO/GCE without cleaning the electrode surface between runs. While the variation of the DA oxidation peak current was less than 1.8 % in buffered solution of pH 2.0, more than 8.4 % reduction of DA peak current was observed in in buffered solution of pH 7.0. Moreover, for the DPVs of 100 μM DA recorded in

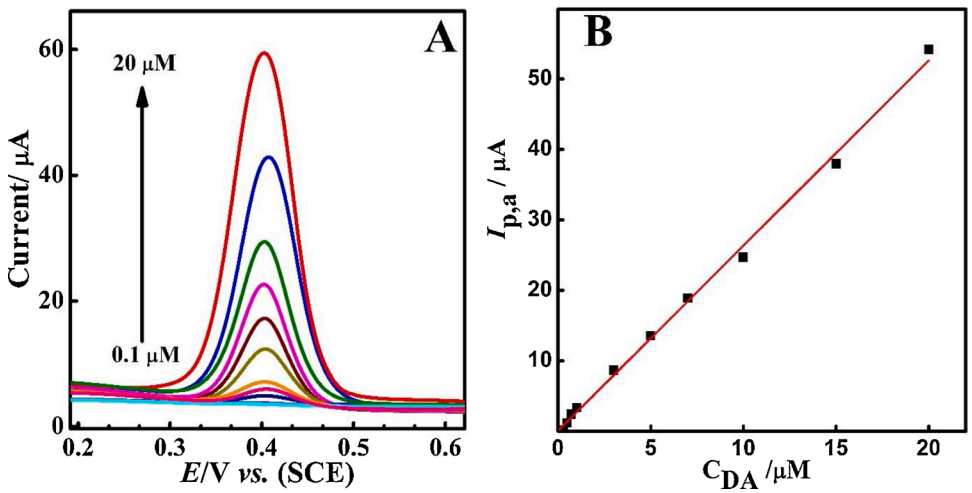

Fig. 10. (A) DPVs for various concentrations of DA in the range of (down to up) 0.1–20 μM in 0.04 M BR solution (pH 2.0), (B) The linear calibration plot of $I_{p,a}$ versus DA concentration, for 50-Cu/ZnO/GCE.

buffered solution of pH 2.0 and 7.0, the width at half-height of oxidation peak was about 80 and 140 mV, respectively. Notably, the narrower peaks provide measurements that are more sensitive and interference free in real samples containing various compounds. In conclusion, for DA analysis using the 50-Cu/ZnO/GCE, the buffered solutions with lower pH are more favorable due to higher repeatability and stability of the voltammograms.

3.5. Effect of the potential scan rate

The CVs of 100 μM DA were recorded at various sweep rates in the range of 0.025 to 0.4 mV to find the nature of its redox process on the surface of 50-Cu/ZnO/GCE, Fig. 9A. Fig. 9B shows that the anodic and cathodic peak currents varied linearly with the square root of scan rate. Also, good linear relationship was observed between logarithm of peak current and logarithm of scan rate with the slop of 0.59, Fig. 9C, revealing that the redox reaction of DA is mainly controlled by diffusion of target analyte towards the 50-Cu/ZnO/GCE surface with a small contribution of adsorption process. Also, the both oxidation and reduction peaks of DA were observed in the all range of evaluated scan rates for which the $I_{p,c}/I_{p,a}$ was about 0.8 to 0.89 with the average value of 0.84. The peaks potential was almost constant and did not shifted by changing scan rate that confirms the completely reversible process for the DA oxidation in the buffered solution of pH 2 on the surface of 50-Cu/ZnO/GCE.

3.6. Voltammetric determinations

As a powerful technique, DPV was employed for the analysis of different concentrations of DA using 50-Cu/ZnO/GCE, Fig. 10A. The resulted calibration plot showed a linear relationship between the oxidation peak current ($I_{p,a}$) and DA concentration (C) over linear dynamic range of 0.1–20 μM, Eq. 3, Fig. 10B. The DA concentration of 55 nM was obtained as the detection limit (S/N = 3). Also, the response stability and repeatability of the 50-Cu/ZnO/GCE were examined using DPV technique. The repeatability of the fabricated modified electrode was tested through recording five sequential DPVs using a same 50-Cu/ZnO/GCE in a 5.0 μM DA solution. The amount of 3.8 % was obtained for relative standard deviation of the peak currents of obtained DPVs. Also, the 50-Cu/nO/GCE retained more than 94 % of its voltammetric response after two weeks storing in room temperature at the laboratory. The stability of the 50-Cu/ZnO nanomaterial helped to reach a stable sensor that can be stored in the room condition for a long time, without the need for any special consideration. In addition, the developed sensor was examined for the analysis real samples such as human serum and the obtained results did not show sensible deviation from the standard solutions of DA. Regarding the simplicity of the electrode modification process, (drop casting of the modifier suspension), the reproducibility of the electrode construction was desirable for which a maximum of 5 % relative standard deviation in peak current was obtained for DA solutions of 5.0 μM. These results confirm the acceptable repeatability and stability of the fabricated modified electrode that can be used for accurate analysis of DA in the real samples.

$$I_{p,a}\ (\mu A) = 2.63\ C_{DA}\ (\mu M) + 0.063 (R^2 = 0.997) \quad (3)$$

The obtained analytical parameters such as sensitivity, detection limit and linear range of the presented sensor towards the determination of DA are compared with earlier reported literature as given in Table 1. From the literature results, it can be observed that the proposed Cu/ZnO sensor showed good comparable analytical parameters than the reported dopamine sensors. It may be attributed to the excellent electrocatalytic activity of the present sensor for high sensitivity and stability in a wide range pH.

The obtained analytical parameters such as sensitivity, detection limit and linear range of the herein described sensor for determination of DA are compared with earlier reported literature as given in Table 1. Here, it can be observed that our Cu/ZnO sensor showed similar linear response ranges, and detection limits as other non-enzymatic sensors for electrochemical detection of DA. Notably, the Cu/ZnO/GCE presented here showed excellent electrocatalytic activity, leading to high sensitivity and stability in a wide range of pH values (e.g. 2–8). The high

Table 1
Linear sensing range, sensitivity, and detection limit of recent dopamine sensors.

Sensor	Linear range (μM)	Sensitivity (nA/μM)	Detection limit (μM)	Ref.
ZnO/CuO composition	1.0–8000	0.09	1.0	[32]
GCE/PANI-ZnO	0.2–2.4	78	0.016	[16]
ZnO–RGO/GCE	0.1–100 200–1800	317.8 28.6	0.063	[33]
CsZnO–PANI/GCE	20–180	13	0.21	[34]
PWA–ZnO NFs/Pt	0.19–450	62.36	0.089	[35]
ZnO/carbon nanofiber	4–20	–	0.402	[18]
Cu/ZnO/GCE	0.1–20	2630	0.055	In this work

sensitivity observed (2630 nA/mM) greatly outperformed previously reported electrodes (0.09–317.8 nA/mM). Here, we believe that the modification of the GCE surface using ZnO is helpful in eliminating the interfering species as well as improving the Faradaic response of desired analyte, while increasing the active surface area. In this case, the simple drop casting of the 50-Cu/ZnO suspension on the GCE surface creates additional electrochemical active surface area (EASA) that enhances the intrinsic activity of the sensor. This phenomenon originates from the nano nature, where smaller amount of finer particle size can increase the number of surface particles exposed to the reaction. Notably, introducing the Cu doped-ZnO nanomaterial to the GCE surface not only increased the EASA, but also facilitated the diffusion process of the analytes toward electrode surface where the redox reaction occurs. Similar observations have been reported when micro-structured carbon-nanotubes electrodes have been employed for electrochemical detection of hydrogen peroxide in aqueous environments [43]. In addition, the shift of redox peak potentials of DA to less positive values when using the 50-Cu/ZnO/GCE electrode indicate a decrease in difference between the oxidation and reduction peak potentials (ΔE_p) compared to the bare GCE, which is highly beneficial. That is the larger the shift in peak potential indicates the faster charge transfer from DA to the electrode. Notably, the electrochemical activation of the 50-Cu/ZnO/GCE in alkaline solution by sweeping potential, significantly improved the DA oxidation (Fig. 5). The higher catalytic activity observed after activation may be due to the formation of droxyl functional groups on the 50-Cu/ZnO surface that facilitate the DA interaction with electrode surface. The oxidation of DA at lower potential on 50-Cu/ZnO/GCE improved the sensing selectivity and helped to overcome the potential interference of other electroactive biomolecules present in real samples. Moreover, the choice of electrochemical technique for the analysis can influence the sensor selectivity. Here, DPV was selected to aid in discriminating the DA oxidation peak from possible interferences.

4. Conclusion

In this study, we developed a highly sensitive DA sensor based on Cu/ZnO composites. These composites were synthesized by a green and simple hydrothermal method and characterized by XRD and SEM. Addition of Cu on ZnO structures changes the morphology and electrochemical response to DA. The fabricated sensor by incorporating the Cu/ZnO powders on GCE showed high sensitivity, broad linear region, good stability, reproducibility and repeatability. The sensor is easily fabricated by cost effective procedure and could be used for usual determining of DA in biological systems. The desirable sensing performance of the Cu/ZnO nanostructures toward DA electro-oxidation revealed the potential of the nonprecious metal oxides specially their hybrids for utilization as a suitable candidate for development of electrochemical biosensors for medical diagnostic purposes.

Declaration of Competing Interest

The authors declare that they have no known competing financial interests or personal relationships that could have appeared to influence the work reported in this paper.

Acknowledgement

This work was supported by Shahid Rajaee teacher Training University.

References

[1] X. Zheng, Y. Guo, J. Zheng, X. Zhou, Q. Li, R. Lin, Simultaneous determination of ascorbic acid, dopamine and uric acid using poly(l-leucine)/DNA composite film modified electrode, Sens. Actuators B Chem. 213 (2015) 188–194, https://doi.org/10.1016/j.snb.2014.11.008.

[2] G. She, X. Huang, L. Jin, X. Qi, L. Mu, W. Shi, SnO_2 nanoparticle-coated ZnO nanotube arrays for high-performance electrochemical sensors, Small 10 (2014) 4685–4692, https://doi.org/10.1002/smll.201401471.

[3] S.S. Kumar, J. Mathiyarasu, K.L. Phani, Exploration of synergism between a polymer matrix and gold nanoparticles for selective determination of dopamine, J. Electroanal. Chem. 578 (2005) 95–103, https://doi.org/10.1016/j.jelechem.2004.12.023.

[4] C.-L. Sun, C.-T. Chang, H.-H. Lee, J. Zhou, J. Wang, T.-K. Sham, W.-F. Pong, Microwave-assisted synthesis of a core– shell MWCNT/GONR heterostructure for the electrochemical detection of ascorbic acid, dopamine, and uric acid, ACS Nano 5 (10) (2011) 7788–7795, https://doi.org/10.1021/nn2015908.

[5] R. Brisch, A. Saniotis, R. Wolf, H. Bielau, H.-G. Bernstein, J. Steiner, B. Bogerts, K. Braun, Z. Jankowski, J. Kumaratilake, M. Henneberg, T. Gos, The role of dopamine in schizophrenia from a neurobiological and evolutionary perspective: old fashioned, but still in Vogue, Front. Psychiatry 5 (2014) 110, https://doi.org/10.3389/fpsyt.2014.00110.

[6] A.S. Adekunle, B.O. Agboola, J. Pillay, K.I. Ozoemena, Electrocatalytic detection of dopamine at single-walled carbon nanotubes-iron (III) oxide nanoparticles platform, Sens. Actuators B Chem. 148 (2010) 93–102, https://doi.org/10.1016/j.snb.2010.03.088.

[7] S. Bilal, A. Akbar, A.-u-H. Ali Shah, Highly selective and reproducible electrochemical sensing of ascorbic acid through a conductive polymer coated electrode, Polymers (Basel). 11 (8) (2019) 1346–1362, https://doi.org/10.3390/polym11081346.

[8] S.K. Ponnaiah, P. Periakaruppan, B. Vellaichamy, New Electrochemical Sensor Based on a Silver-Doped Iron Oxide Nanocomposite Coupled with Polyaniline and Its Sensing Application for Picomolar-Level Detection of Uric Acid in Human Blood and Urine Samples, J. Phys. Chem. B 122 (2018) 3037–3046, https://doi.org/10.1021/acs.jpcb.7b11504.

[9] Y. Li, Q. Lu, A. Shi, Y. Chen, S. Wu, L. Wang, Electrochemical determination of dopamine in the presence of ascorbic acid and uric acid using the synergistic effect of gold nanoflowers and L-cysteamine monolayer at the surface of a gold electrode, Anal. Sci. 27 (9) (2011) 921–927, https://doi.org/10.2116/analsci.27.921.

[10] N.F. Atta, A. Galal, D.M. El-Said, Novel Design of a Layered Electrochemical Dopamine Sensor in Real Samples Based on Gold Nanoparticles/β-Cyclodextrin/Nafion-Modified Gold Electrode, ACS Omega 4 (19) (2019) 17947–17955, https://doi.org/10.1021/acsomega.9b01222.

[11] K. Chen, W. Chou, L. Liu, Y. Cui, P. Xue, M. Jia, Electrochemical Sensors Fabricated by Electrospinning Technology: An Overview, Sensors (Basel). 19 (17) (2019) 3676–3694, https://doi.org/10.3390/s19173676.

[12] A. Walcarius, S.D. Minteer, J. Wang, Y. Lin, A. Merkoçi, Nanomaterials for bio-functionalized electrodes: recent trends, J. Mater. Chem. B 38 (2013) 4867–5164, https://doi.org/10.1039/c3tb20881h.

[13] L.-L. Gao, W.-J. Sun, Y.Ran X-Mei, B.En-Q. Gao, Graphite paste electrodes modified with a sulfo-functionalized metal-organic framework (type MIL-101) for voltammetric sensing of dopamine, Microchimica Acta 186 (2019) 762, https://doi.org/10.1007/s00604-019-3943-2.

[14] Z. Tavakolian-Ardakani, O. Hosu, C. Cristea, M. Mazloum-Ardakani, G. Marrazza, Latest trends in electrochemical sensors for neurotransmitters: a Review, Sensors (Basel). 19 (9) (2019) 2037, https://doi.org/10.3390/s19092037.

[15] K.J. Stine, Biosensor applications of electrodeposited nanostructures, Appl. Sci. 9 (2019) 797, https://doi.org/10.3390/app9040797.

[16] O.E. Fayemi, A.S. Adekunle, B.E. Kumara Swamyd, E.E. Ebenso, Electrochemical sensor for the detection of dopamine in real samples using polyaniline/NiO, ZnO, and Fe3O4 nanocomposites on glassy carbon electrode, J. Electroanal. Chem. 818 (2018) 236–249, https://doi.org/10.1016/j.jelechem.2018.02.027.

[17] D. Balram, K.-Y. Lian, N. Sebastian, A novel electrochemical sensor based on flower shaped zinc oxide nanoparticles for the efficient detection of dopamine, Int. J. Electrochem. Sci. 13 (2018) 1542–1555, https://doi.org/10.20964/2018.02.06.

[18] C. Yang, C. Zhang, T. Huang, X. Dong, L. Hua, Ultra-long ZnO/carbon nanofiber as free-standing electrochemical sensor for dopamine in the presence of uric acid, J. Mater. Sci. 5 (2019) 14897–14904, https://doi.org/10.1007/s10853-019-04000-x.

[19] W.-H. Zhou, H.-H. Wang, W.T. Li, X.-C. Guo, D.-X. Kou, Z.-J. Zhou, Y.-N. Meng, Q.-W. Tian, S.-X. Wu, Gold Nanoparticles Sensitized ZnO Nanorods Arrays for Dopamine Electrochemical Sensing, J. Electrochem. Soc. 165 (2018) G3001–G3007, https://doi.org/10.1149/2.0011811jes.

[20] R. Ahmad, M.S. Ahn, Y.B. Hahn, Fabrication of a non-enzymatic glucose sensor field-effect transistor based on vertically-oriented ZnO nanorods modified with Fe_2O_3, Electrochem. commun. 77 (2017) 107–111, https://doi.org/10.1016/j.elecom.2017.03.006.

[21] H.M. Mali, S.S. Narwade, Y.H. Navale, S.B. Tayade, R.V. Digraskar, V.B. Patil, A. S. Kumbhar, B.R. Sathe, Heterostructural CuO−ZnO Nanocomposites: A highly selective chemical and electrochemical NO_2 sensor, ACS Omega 4 (2019) 20129–20141, https://doi.org/10.1021/acsomega.9b01382.

[22] D.U.J. Jung, R. Ahmad, Y.B. Hahn, Nonenzymatic flexible field-effect transistor based glucose sensor fabricated using NiO quantum dots modified ZnO nanorods, J. Colloid Interface Sci. 512 (2018) 21–28, https://doi.org/10.1016/j.jcis.2017.10.037.

[23] S. Drexler, J. Faria, M.P. Ruiz, J.H. Harwell, D.E. Resasco, Amphiphilic nanohybrid catalysts for reactions at the water/oil interface in subsurface reservoirs, Energy Fuels 26 (2012) 2231–2241, https://doi.org/10.1021/ef300119p.

[24] D. Santhanaraj, M.P. Ruiz, M.R. Komarneni, T. Pham, G. Li, D.E. Resasco, J. Faria, Synthesis of α,β- and β-Unsaturated Acids and Hydroxy Acids by Tandem Oxidation, Epoxidation, and Hydrolysis/Hydrogenation of Bioethanol Derivatives,

Angew. Chemie - Int. Ed. 59 (2020) 1–6, https://doi.org/10.1002/anie.202002049.
[25] M. Behrens, F. Studt, I. Kasatkin, S. Kühl, M. Hävecker, F. Abild-pedersen, S. Zander, F. Girgsdies, P. Kurr, B. Kniep, M. Tovar, R.W. Fischer, J.K. Nørskov, R. Schlögl, The Active Site of Methanol Synthesis over Cu/ZnO/Al2O3 Industrial Catalysts, Science (80-.) 336 (2012) 893–898, https://doi.org/10.1126/science.1219831.
[26] S.G. Jadhav, P.D. Vaidya, B.M. Bhanage, J.B. Joshi, Catalytic carbon dioxide hydrogenation to methanol: a review of recent studies, Chem. Eng. Res. Des. 92 (2014) 2557–2567, https://doi.org/10.1016/j.cherd.2014.03.005.
[27] Y. Zhuang, M. Zhao, Y. He, F. Cheng, S. Chen, Fabrication of ZnO/rGO/PPy heterostructure for electrochemical detection of mercury ion, J. Electroanal. Chem 826 (2018) 90–95, https://doi.org/10.1016/j.jelechem.2018.08.016.
[28] S. Hemmati, A. Anaraki Firooz, A.A. Khodadadi, Y. Mortazavi, Nanostructured SnO2-ZnO sensors: highly sensitive and selective to ethanol, Sensors Actuators, B Chem. 160 (2011) 1298–1303, https://doi.org/10.1016/j.snb.2011.09.065.
[29] Z. Zhu, L. Qu, Y. Guo, Y. Zeng, W. Sun, X. Huang, Electrochemical detection of dopamine on a Ni/Al layered double hydroxide modified carbon ionic liquid electrode, Sensors Actuators, B Chem. 151 (2010) 146–152, https://doi.org/10.1016/j.snb.2010.09.032.
[30] A. Anaraki Firooz, M. Keyhani, The effect of different dopants (Cr, Mn, Fe, Co, Cu and Ni) on photocatalytic properties of ZnO nanostructures, Int. J. Nanosci. Nanotechnol. 16 (2020) 59–65.
[31] R. Ahmad, N. Tripathy, M.S. Ahn, K.S. Bhat, T. Mahmoudi, Y. Wang, J.Y. Yoo, D. W. Kwon, H.Y. Yang, Y.B. Hahn, Highly efficient non-enzymatic glucose sensor based on CuO modified vertically-grown ZnO nanorods on electrode, Sci. Rep. 7 (2017) 5715, https://doi.org/10.1038/s41598-017-06064-8.
[32] K. Khun, Z.H. Ibupoto, X. Liu, N.A. Mansor, A.P.F. Turner, V. Beni, M. Willander, An Electrochemical Dopamine Sensor Based on the ZnO/CuO Nanohybrid Structures, J. Nanosci. Nanotechnol. 14 (2014) 6646–6652, https://doi.org/10.1166/jnn.2014.9367.
[33] L. Zhihua, Z. Xuchenga, W. Kunb, Z. Xiaoboa, S. Jiyong, H. Xiaowei, M. Holmes, A novel sensor for determination of dopamine in meat based on ZnO-decorated reduced graphene oxide composites, Innov. Food Sci. Emerg. Technol. 31 (2015) 196–203, https://doi.org/10.1016/j.ifset.2015.06.011.
[34] K. Pandiselvi, S. Thambidurai, Chitosan–ZnO/polyanilne nanocomposite modified glassy carbon electrode for selective detection of dopamine, Int. J. Boil. Macromol 67 (2014) 270–278, https://doi.org/10.1016/j.ijbiomac.2014.03.028.
[35] J. Wu, F. Yin, Studies on the electrocatalytic oxidation of dopamine at phosphotungstic acid–ZnO spun fiber-modified electrode, Sens. Act. B: Chem. 185 (0) (2013) 651–657, https://doi.org/10.1016/j.snb.2013.05.052.
[36] M. Ghalkhani, B. Hosseini nia, J. Beheshtian, A. Anaraki Firooz, Synthesis of undoped and Fe nanoparticles doped SnO_2 nanostructure: study of structural, optical and electrocatalytic properties, J Mater Sci: Mater Electron. 28 (2017) 7568–7574, https://doi.org/10.1007/s10854-017-6448-y.
[37] M.H. Darvishnejad, A. Anaraki Firooz, J. Beheshtian, A.A. Khodadadi, Highly sensitive and selective ethanol and acetone gas sensors by adding some dopants (Mn, Fe, Co, Ni) onto hexagonal ZnO plates, RSC Adv. 6 (2016) 7838–7845, https://doi.org/10.1039/C5RA24169C.
[38] A. Akbari, A. Anaraki Firooz, J. Beheshtian, A.A. Khodadadi, Experimental and theoretical study of CO adsorption on the surface of single phase hexagonally plate ZnO, App. Surf. Sci. 315 (2014) 8–15, https://doi.org/10.1016/j.apsusc.2014.07.034.
[39] D. Rossouw, P. Burdet, F. De La Peña, C. Ducati, B.R. Knappett, A.E.H. Wheatley, P. A. Midgley, Multicomponent Signal Unmixing from Nanoheterostructures: Overcoming the Traditional Challenges of Nanoscale X-ray Analysis via Machine Learning, Nano Lett. 15 (2015) 2716–2720, https://doi.org/10.1021/acs.nanolett.5b00449.
[40] Y.X. Li, X. Huang, Y.L. Chen, L. Wang, X.Q. Lin, Simultaneous determination of dopamine and serotonin by use of covalent modification of 5-hydroxytryptophan on glassy carbon electrode, Microchimica Acta 164 (1-2) (2009) 107–112, https://doi.org/10.1007/s00604-008-0040-3.
[41] W. Zhang, J. Zheng, J. Shi, Z. Lin, Q. Huang, H. Zhang, C. Yi Wei, J. Chen, S. Hu, A. Hao, Nafion covered core– shell structured Fe_3O_4@graphene nanospheres modified electrode for highly selective detection of dopamine, Anal. Chim. Acta 853 (0) (2015) 285–290, https://doi.org/10.1016/j.aca.2014.10.032.
[42] M.L. Mohd Napi, S.M. Sultan, R. Ismail, K.W. How, M.K. Ahmad, Electrochemical-based biosensors on different zinc oxide nanostructures: a review, Materials 12 (18) (2019) 2985, https://doi.org/10.3390/ma12182985.
[43] B.J. Brownlee, K.M. Marr, J.C. Claussen, B.D. Iverson, Improving sensitivity of electrochemical sensors with convective transport in free-standing, carbon nanotube structures, Sensors Actuators, B Chem. 246 (2017) 20–28, https://doi.org/10.1016/j.snb.2017.02.037.